ORIGINAL PAPER

Immobilization and direct electrochemistry of cytochrome *c* at a single-walled carbon nanotube-modified electrode

Yajing Yin · Ping Wu · Yafen Lü · Pan Du · Yanmao Shi · Chenxin Cai

Abstract A single-walled carbon nanotube (SWNT)-modified electrode was fabricated and characterized by SEM and ac impedance techniques. The direct electrochemistry of cytochrome *c* (Cyt *c*), which was adsorbed on the surface of the SWNT, was studied by cyclic voltammetry. The results from cyclic voltammetry and infrared spectroscopy indicated that Cyt *c* remained in its original structure and did not undergo structural change after its immobilization on the SWNT. Further results demonstrated that the SWNT had promotional effects on the direct electron transfer of Cyt *c* and also indicated that the immobilized Cyt *c* retained its electrocatalytic activity to the reduction of H_2O_2. This modified electrode might be used in development of new biosensors and the biofuel cells.

Keywords Carbon nanotube · Electrochemical properties · Catalytic properties · Biocompatibility

Introduction

Electron transfer in biological systems is one of the leading areas in biochemical and biophysical sciences. In the past few years, there had been considerable interest in direct electron transfer between the redox proteins (enzymes) and the electrode surfaces [1–5]. Many factors, however, can impede direct electron transfer of redox proteins (enzymes) at the surface of electrodes. Those factors include burying of electroactive groups deep within the overall structure, adsorption on electrode surfaces of macromolecular species (impurities) or denatured forms of proteins themselves, and unfavorable (thus unproductive) approaches to the electrode. Generally speaking, the properties of electrode surface, which include charge density, hydrophilicity, and strength of interaction, may be important for developing a well-marked response. For the applications in the biosensors, the proteins (enzymes) should be immobilized on the electrode surface to avoid many complications linked to the solution systems. Many immobilization methods were developed to fabricate protein (enzymes) electrodes, such as sol–gel [6–8] and self-assembled techniques [9–11], etc. From these studies, one could obtain valuable information on the mechanisms of biological electron transfer and further develop the electrocatalytic system.

Cytochrome *c* (Cyt *c*) is a very basic, heme-containing redox protein with a molecular weight of ca. 12,300 g/mol and approximately spherical shape with 34 Å in diameter [12]. The structural and dynamic properties of this water-soluble heme protein had been known in great detail [13, 14]. It functions as an electron carrier in aerobic respiration, transferring electrons from Cyt *c* reductase to Cyt *c* oxidase where the electrons are utilized to reduce oxygen to water. The reaction partners of Cyt *c* are membrane-bound enzyme complexes integrated in the mitochondrial membrane in close vicinity to each other, and Cyt *c* most likely migrates between both reaction sites via lateral diffusion along the membrane surface. Generally, an investigation of the electron transfer of Cyt *c* at electrode/solution interfaces may contribute in particular a better understanding of the natural redox process of this protein and, possibly, the identification of the parameters governing interfacial charge-transfer processes. Progress in achieving direct electron transfer has been gained by using carefully cleaned electrodes [15, 16] and purified protein samples [17], or by the modification of the electrode surface via promoters

Y. Yin · P. Wu · Y. Lü · P. Du · Y. Shi · C. Cai (✉)
Department of Chemistry, Jiangsu Key Laboratory for Molecular and Medical Biotechnology, Nanjing Normal University, Nanjing 210097, People's Republic of China
e-mail: cxcai@njnu.edu.cn

which are able to help the electron transfer [18, 19]. Many attempts have been made to mimic biomembranes as in physiological systems using lipid bilayers on freshly cleaved platinum or gold wires, or lipid layer-coated electrodes [20, 21]. However, due to its importance, the direct electron transfer of Cyt *c* is still a vital topic of investigation.

Recently, modifying the electrode surface with nanoparticles allowed efficient electron transfer between the electrode and redox proteins (enzymes). This was effective in understanding the redox properties of proteins (enzymes) and more importantly, in developing biosensors and the related apparatus without mediators or promoters [22, 23]. Especially, carbon nanotubes (CNTs), which were found in two types of structures: multiwalled carbon nanotube (MWNT) and single-walled carbon nanotube (SWNT), have gained considerable attention in recent years for this purpose [24, 25] because of their remarkable electronic and mechanical properties. The closed topology and the tubular structure of CNTs make them unique among different carbon forms and provide useful pathways for chemical studies [26–28]. Certainly, in studies of the electrochemical properties of biologically relevant molecules such as hydrogen peroxide [29–31], NAD(P)H [32–34], and dopamine [31, 35–38], etc., CNT-modified electrodes have shown superior performances as compared to other carbon electrodes. Also, their subtle electronic properties suggest that CNTs have the stability to promote the direct electron transfer reaction of some important biomolecules, such as microperoxidase 11 [39], horseradish peroxidase [40, 41], hemoglobin [42], and glucose oxidase [43–45], etc. In this work, Cyt *c* was immobilized on the surface of SWNT by adsorption and characterized by SEM and Raman and IR spectroscopy. Voltammetric results indicated that Cyt *c* could undergo the direct electron transfer reaction and remained the electrocatalytic activities to the reduction of H_2O_2. Comparing to the previous work [46], which showed that the direct electron transfer of Cyt *c*, which was in solution, could only be achieved on electrochemically activated SWNT, the present work indicated that the unactivated SWNT could also facilitate the direct electron transfer of Cyt *c* when it was immobilized on the surface of SWNT. The method presented in this study may be more useful in the development of reagentless biosensor than that Cyt *c* in solution.

Experimental

Chemicals

Horse heart Cyt *c* (type VI) was obtained from Sigma (St. Louis, MO, USA) and used without further purification. A 30% hydrogen peroxide solution was purchased from Shanghai Chemical Reagent (Shanghai, China), and a fresh solution of H_2O_2 was prepared daily. SWNTs (<2 nm in diameter with purity of >90%) were purchased from Shenzhen Nanotech Port (Shenzhen, China). Before use, they were treated by refluxing in 3 M HNO_3 for 3 h, filtered with a minipore size membrane (pore size was 0.22 μm in diameter, Anpel), then thoroughly washed with water and finally dried under vacuum at 60 °C overnight to obtain purified SWNT. Such SWNT had functional surfaces, such as –OH and –COOH groups, which could be characterized by IR spectroscopy. All other chemicals were of analytical grade. All the solutions were prepared with doubly distilled water. The 0.1 M phosphate buffer solutions (PBS, pH 7.0), which were made up from Na_2HPO_4 and NaH_2PO_4, were always employed as supporting electrolyte.

Fabrication of SWNT/GC electrode and the immobilization of Cyt *c*

The glassy carbon (GC) electrode (3 mm in diameter) was polished sequentially with metallographic abrasive paper (No. 6), slurries of 0.3 and 0.05-μm alumina, to mirror finish. After rinsed with doubly distilled water, it was sonicated with absolute ethanol and doubly distilled water for about 1 min, respectively.

The fabrication of SWNT/GC electrode and the immobilization Cyt *c* are summarized as follows: 1 mg of purified SWNT was dispersed in 2 ml dimethylformamide (DMF) with the aid of ultrasonication to give a 0.5-mg/ml black suspension. The surface of the well-polished GC electrode was treated by a dropping of suspension (2 μl) of SWNT in DMF and then dried under an infrared lamp. The obtained SWNT/GC electrode was thoroughly rinsed with water and immersed in a 5-mg/ml (ca. 0.4 mM) Cyt *c* in 0.1 M PBS at 4 °C overnight to acquire the Cyt *c*-SWNT/GC electrode. Then, Cyt *c*-SWNT/GC electrode was taken out from Cyt *c* solution and washed thoroughly with distilled water to remove the unadsorbed Cyt *c* molecules. In case that it was not used immediately, the electrode was stored at 4 °C in a refrigerator.

Apparatus

The scanning electron microscopic (SEM) images of SWNT on GC electrode surface were obtained with a LEO 1530 VP Field-Emission Scanning Electron Microscope (German). Reflection–absorption infrared (RAIR) spectra were recorded using a Nexus 670 FT-IR spectrophotometer (Nicolet Instrumental, USA) with the resolution of 4 cm^{-1}. The micro-Raman spectrum was recorded with a Labram HR 800 UV (Jobin Yvon) Raman spectrometer at the ambient temperature using 514.5-nm excitation and a spectral slit width of 2 cm^{-1}.
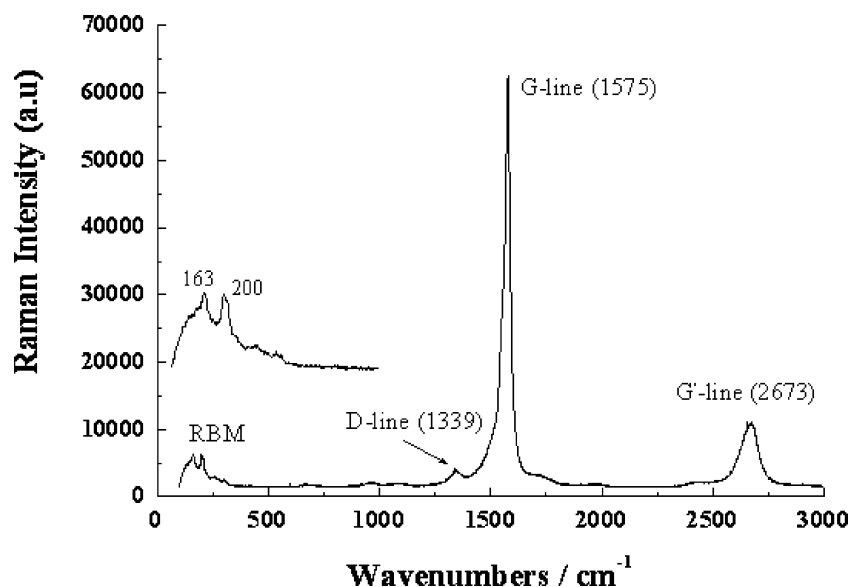
Fig. 1 A typical Raman spectrum (excited with 514.5 nm laser) of the SWNT

The electrochemical experiments were carried out with a CHI660B electrochemical workstation (CH Instruments, USA) with a conventional three-electrode cell. A Cyt *c*-SWNT/GC electrode was used as the working electrode. The coiled Pt wire and the saturated calomel electrode (SCE) were used as the counter electrode and the reference electrode, respectively. Buffers were purged with high-purity nitrogen for at least 30 min before experiments, and a nitrogen environment was then kept over solutions in the cell to protect the solution from oxygen. All experiments were performed at the room temperature (22±2 °C).

Results and discussions

Electrode characterization

Raman spectroscopy has been considered to be one of the most powerful tools for characterization of carbon nanotube
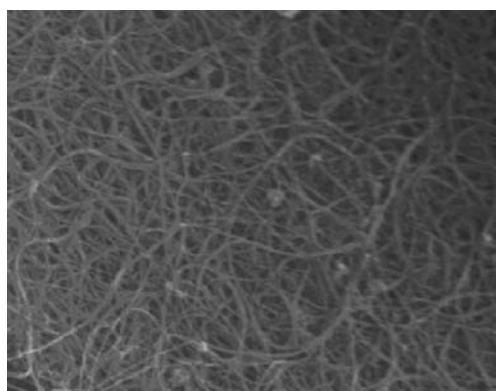

Fig. 2 SEM image of SWNT on the surface of GC electrode

[47]. Raman spectra of CNT have been extensively studied and are now rather well understood [47–49]. Without sample preparation, a fast and nondestructive analysis is possible. Figure 1 showed a typical Raman spectrum of the SWNT used for electrode fabrication. A strong peak appeared at 1,575 cm^{-1}, which was associated with the *G*-band, corresponding to the E_{2g} stretching mode of graphite [50]. The appearance of peak at 1,339 cm^{-1}, the so-called *D*-line, indicated the residual ill-organized graphite (amorphous carbon) in SWNT sample even though the sample had been purified with HNO$_3$. The integrated relative intensities of the *D* mode vs the graphitic *G* mode (*G/D* >50) showed, however, that only a minor fraction of amorphous carbon presented in the sample and the purity of the SWNT sample was high. The peak at 2,673 cm^{-1} (often called *G*′-line) is usually assigned to the first overtone of the *D* mode. In the low-frequency region, there were two main peaks at about 163 and 200 cm^{-1}, assigned to A_{1g} radial breathing mode (RBM) of SWNT, whose frequency depended essentially on the diameter of the tube. According to the relationship between the RBM frequency and the tube diameter [51]:

$$d(in\ nm) = 248/\omega(in\ cm^{-1}), \tag{1}$$

these two peaks corresponded to the SWNT diameters of 1.52 and 1.24 nm, respectively.

The SEM image of the SWNT on the surface of a pretreated GC electrode was shown in Fig. 2. It can be seen that the SWNT was formed as bundles, some of which twisted together. From the image, it could also be seen that a negligible amount of amorphous carbon impurities existed in SWNT sample. This conclusion was consistent with that obtained from Raman spectrum.
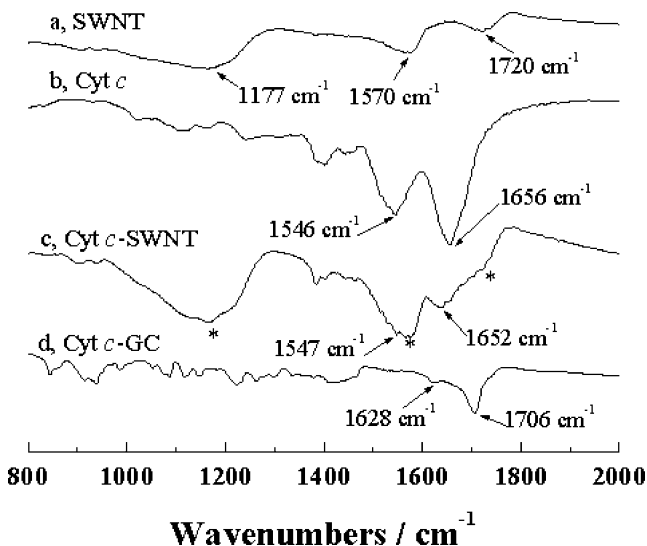
Fig. 3 RAIR spectra of SWNT (**a**), free Cyt *c* (**b**), Cyt *c* immobilized on the surface of SWNT (Cyt *c*-SWNT, **c**) and on the surface of bare GC electrode (Cyt *c*-GC, **d**)

RAIR is a surface infrared technique ideally suited to exploring the secondary structure of proteins (enzymes) on a solid substrate surface [52]. To confirm the existence of Cyt *c* on the surface of SWNT and the Cyt *c* remaining in its original structure after being adsorbed, RAIR experiments were carried out. The results were presented in Fig. 3. In proteins (enzymes), although the peptide bonds –CO–NH– have several distinct vibrational modes, amide I (1,700–1,600 cm^{-1}), which is caused by C=O stretching vibrations of peptide linkages, and amide II (1,620–1,500 cm^{-1}), which results from a combination of N–H in-plane bending and C–N stretching vibrations of the peptide groups, are the most useful modes for estimating the detailed information on the secondary structure (i.e., α-helix and β-sheet) of polypeptide backbone chain [53, 54]. The amide I and II bands of Cyt *c* on the surface of SWNT (Fig. 3c) had similar shapes and positions to that of the free Cyt *c* (not adsorbed on the surface of SWNT, Fig. 3b)
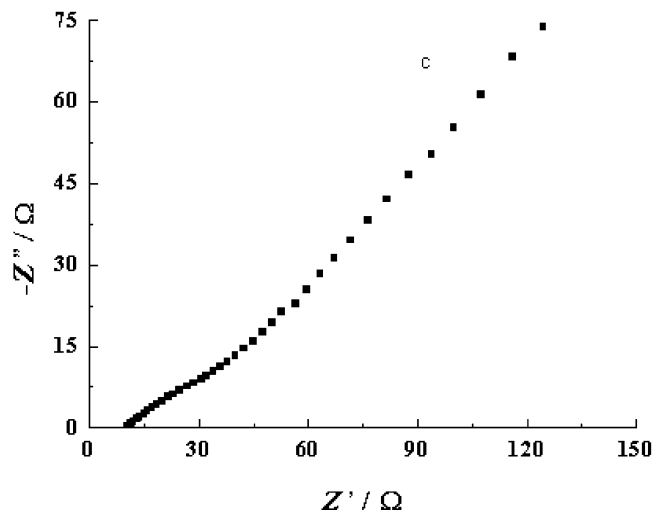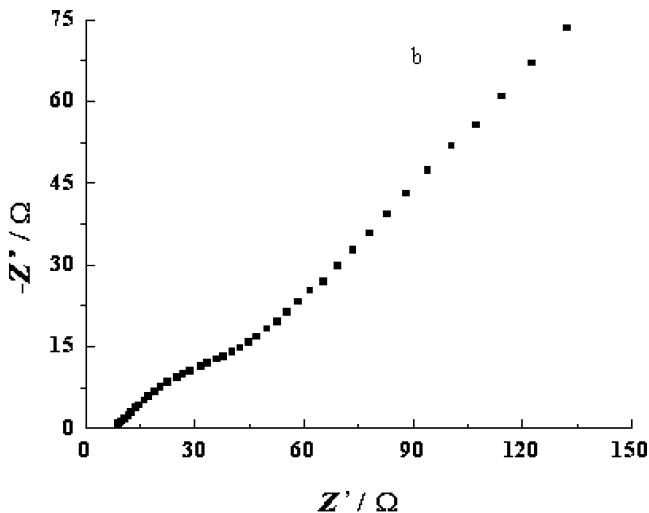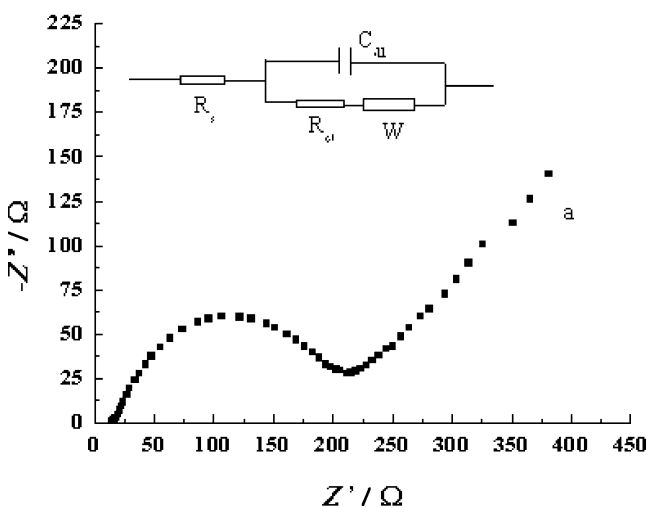
Fig. 4 Nyquist plots for a bare GC electrode (**a**), SWNT/GC electrode (**b**), and Cyt *c*-SWNT/GC electrode (**c**) in presence of 5 mM $Fe(CN)_6^{3-}$/ 5 mM $Fe(CN)_6^{4-}$ in 0.1 M KCl solution. The electrode potential was biased at 0.21 V (vs SCE). The Randles circuit is shown in the inset of (**a**)
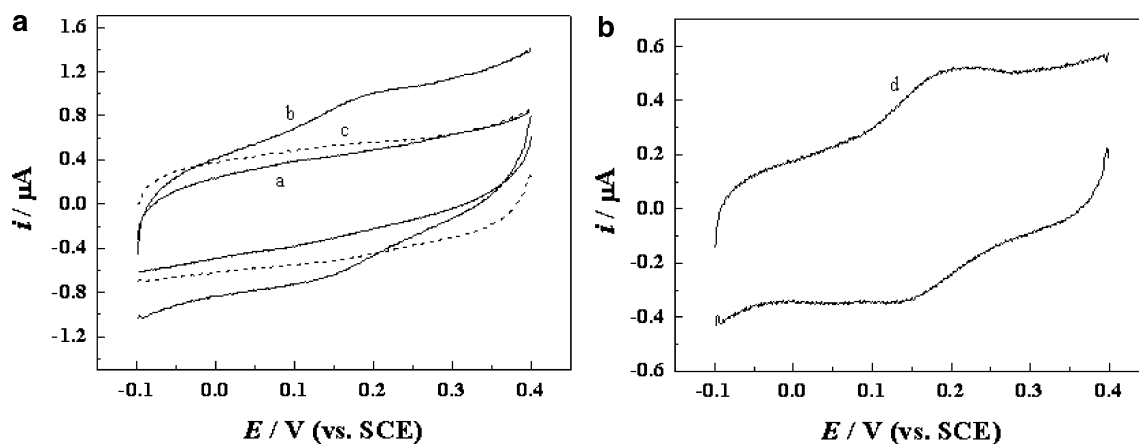
Fig. 5 Cyclic voltammograms of the SWNT/GC (**a**), Cyt *c*-SWNT/GC (**b**), and Cyt *c*/GC (**c**) electrodes in 0.1 M PBS (pH 7.0) at a scan rate of 60 mV/s. Curve **d** is the background-subtracted cyclic voltammogram using the data presented in curve **a** and **b**

except that the bands shifted very slightly (1,656 to 1,652 cm^{-1} and 1,546 to 1,547 cm^{-1} for amide I and II, respectively), which resulted from the interaction between Cyt *c* and SWNT. Figure 3a was the IR spectrum of SWNT. The appearance of the peaks (1,720, 1,570, and 1,170 cm^{-1}) indicated the presence of carboxylic and carboxylate groups on the surface of the SWNT. The oxygen-containing group might be introduced during purification by using HNO$_3$. These peaks of oxygen-containing groups also appeared in Fig. 3c (marked with * in Fig. 3c). The RAIR spectrum of Cyt *c* on the surface of bare GC electrode showed completely different spectral characteristics in amide I and II regions (Fig. 3d). The bands of amide I and II had a great shift (1,656 to 1,706 cm^{-1} and 1,546 to 1,628 cm^{-1}, respectively) compared with that of free Cyt *c*. The above results verified that Cyt *c* was adsorbed on the surface of SWNT and remained in its original structure and also showed that denaturation of Cyt *c* occurred on bare GC electrode surface.

Electrochemical impedance spectroscopy can provide the information on the impedance changes of the electrode surface during the modification process. Figure 4 showed the typical results of ac impedance spectra of the bare GC (a), SWNT/GC (b), and Cyt *c*-SWNT/GC (c) electrodes. The profiles showed a semicircular part at high frequencies corresponding to the electron transfer limited process and a linear part at low frequencies to the diffusion process. To obtain detailed information about the electrode/solution interface, the Randles circuit (inset of Fig. 4a), which was used by Wang et al. [39] for the similar electrode system, was chosen to fit the impedance data obtained. Thus, the electron-transfer resistance, R_{ct}, could be estimated, which equaled 130, 50, and 41 Ω for the bare GC electrode, SWNT/GC electrode, and Cyt *c*-SWNT/GC electrode, respectively. The values of R_{ct} at SWNT/GC and Cyt *c*-SWNT/GC electrodes decreased greatly compared with that of bare GC electrode. This might be due to the subtle

electronic properties of SWNT because it had been proved that carbon nanotube had better conductivity than that for other forms of carbon [55]. Treatment of SWNT with nitric acid (see "Experimental" section) would introduce the carboxylic acid and thus negative charges on the surface of SWNT. Adsorption of Cyt *c* resulted in the decrease of the surface negative charges on SWNT since the isoelectric point of Cyt *c* was about 10 [56] and it carried a positive charge at pH 7.0. Thus, the value of R_{ct} at Cyt *c*-SWNT/GC electrode decreased further compared with that of SWNT/GC electrode (from 50 to 41 Ω), which was similar to the previous reports [12, 57].

Direct electron transfer of Cyt *c*

Figure 5 depicted the typical cyclic voltammograms of the SWNT/GC electrode (curve a) and the Cyt *c*-SWNT/GC electrode (curve b) in 0.1 M PBS (pH 7.0) at a scan rate of 60 mV/s. No redox peak was observed at the SWNT/GC electrode in the potential range of interest, but a pair of redox peaks was obtained at the Cyt *c*-SWNT/GC electrode. The redox peaks were more obvious after subtracting the background (curve d). The anodic (E_{pa}) and cathodic (E_{pc}) peak potentials were 191 and 139 mV, respectively, at a scan rate of 60 mV/s. The formal potential, $E^{0\prime}$, calculated by averaging the cathodic and anodic peak potentials, was found to be 165 mV. The separation of peak potentials, ΔE_p, was 52 mV, and the ratio of cathodic-to-anodic peak currents was nearly in unity. These features were characteristic of the reversible electrode process of the heme Fe^{III}/Fe^{II} redox couple in Cyt *c* molecules, which suggested that the direct electron transfer of Cyt *c* adsorbed on the surface of SWNT could be achieved in spite of its large molecule structure.

If Cyt *c* was immobilized directly on the surface of bare GC electrode, the cyclic voltammogram of the resulted electrode (Cyt *c*/GC) did not appear the redox peaks like
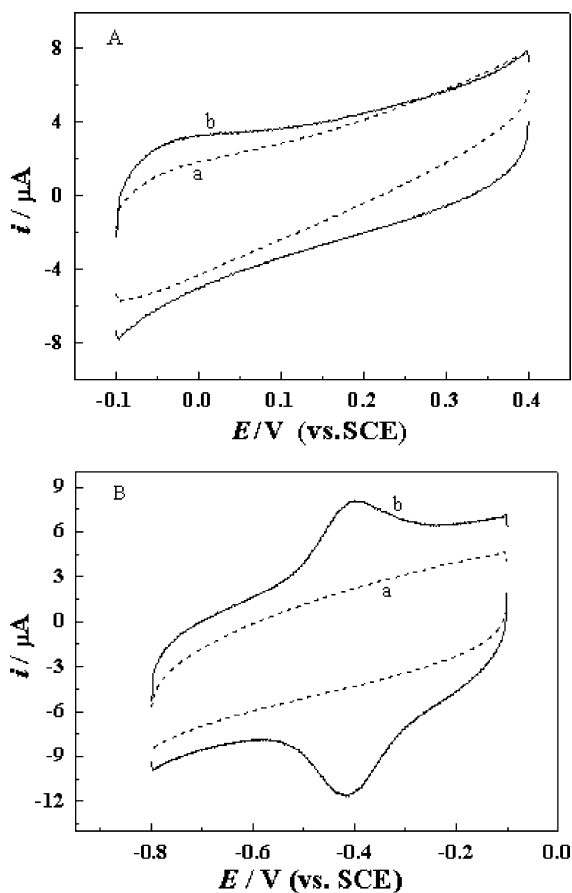
Fig. 6 Cyclic voltammograms of the SWNT/GC electrode (**a**) and the heme-SWNT/GC electrode (**b**) in 0.1 M PBS (pH 7.0) at a scan rate of 60 mV/s

those in curve b (see curve c), suggesting that Cyt *c* had undergone the structure change and might be denatured on the surface of bare GC electrode. This result was consistent with that obtained from RAIR spectra (curve d in Fig. 3). The redox potential of denatured Cyt *c* is much different from the native one and is not in the potential range of Fig. 5 (see below).

The $E^{0'}$ value obtained in this study was very close to that previous reports for Cyt *c* in solution phase [11, 20]. It was also close to that for Cyt *c* immobilized on DNA-modified CNT [56] and for Cyt *c* in the solution phase at an electrochemically activated, CNT-modified GC electrode [46]. However, if Cyt *c* was directly immobilized on the surface of unmodified and unactivated CNT by a method of cyclic scanning, its formal potential had a great shift in negative direction (about −350 mV vs SCE) [12] compared to the value obtained in this work. It had been addressed that electrochemical behavior (e.g., $E^{0'}$) of Cyt *c* was closely relevant to its state [58, 59]. For instance, Cyt *c* in its native state (e.g., those in solution phase or in an adsorbed form without a conformational change) showed a redox process with $E^{0'}$ of ca. 100 mV (vs Ag/AgCl)

[60], while the denatured Cyt *c* exhibited a redox process at ca. −440 mV (vs SCE), for example, on a bare Au electrode [61]. In the case of Cyt *c* adsorbed on the surface of electrode modified with functional films, for example, the self-assembled membrane and the surfactants, Cyt *c* could essentially interact with the films, which avoided its direct adsorption on the bare electrode and, hence, prevented it from being denatured on the modified electrode surface. The interactions between Cyt *c* and bare electrode surface essentially led to structural alternations and the heme crevice, resulting in an open conformation (state II) compared to the closed structure in the native state (state I) of Cyt *c* and thereby a decrease in the redox potential [62]. The state II is also electroactive, but its potential is not in the same potential region as that of the original state since it has undergone structural alternations [58]. To confirm this conclusion, the free heme was directly adsorbed on the surface of SWNT (heme-SWNT/GC electrode) using the same method as preparation of the Cyt *c*-SWNT/GC electrode. The results presented in Fig. 6 indicated that no observable redox response was found in the potential range of −0.1 to 0.4 V (Fig. 6a), whereas there was a symmetrical redox couple at −0.41 V (Fig. 6b). These results showed that the redox response of Cyt *c* reported previously [12] was that of the state II (or might be a denatured state), not the response of the original Cyt *c* (state I).

The redox potentials of the Cyt *c*-SWNT/GC electrode were scan rate dependent. The values of E_{pa} and E_{pc} shifted slightly to the positive and negative directions, respectively, and ΔE_p increased with the increase of the scan rate. However, $E^{0'}$ was almost independent on the scan rates ($E^{0'}$=164 ± 2 mV in the scan rate range of 20 to 200 mV/s). The anodic and cathodic peak currents were of similar magnitude and both of them were linearly proportional to scan rate up to more than 200 mV/s, suggesting that the reaction was a surface-controlled process, which was expected for immobilized systems [63].

The redox peaks of the direct electron transfer of Cyt *c* were almost invariable after the Cyt *c*-SWNT/GC electrode was continuously scanned for a long time (more than 30 min) and showed little change over 7 days of storage in buffer in 4 °C, indicating that the response of the direct electron transfer of Cyt *c* was fairly stable. The stability of the SWNT/GC electrode was also checked by the method of continuous scanning, which showed that cyclic voltammetric response of the electrode remained unchangeable even though the electrode was continuously scanned over 100 scans. The reproducibility of the electrodes, including SWNT/GC and Cyt *c*-SWNT/GC electrode, was studied by comparing the responses of five electrodes, which were prepared from five independent SWNT suspensions (all suspensions with SWNT at 0.5 mg/ml) using the same GC electrode. The reproducibility of the electrodes was also
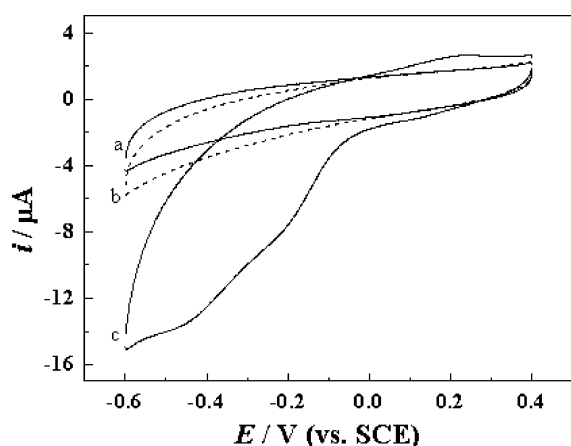
Fig. 7 Cyclic voltammograms of SWNT/GC electrode in 0.1 M PBS (pH 7.0) in the absence (**a**) and presence (**b**) of 5 mM H_2O_2. Curve **c** shows the cyclic voltammogram of Cyt c-SWNT/GC electrode in 0.1 M PBS (pH 7.0) containing 5 mM H_2O_2. Scan rate is 20 mV/s

checked by comparing the responses of five electrodes, which were prepared from the same SWNT suspension (also at 0.5 mg/ml) using five independent GC electrodes (at the same size). The results indicated that the responses of these electrodes were almost the same within the range of experimental errors, and suggested that the procedures of preparation of the SWNT-modified electrode and immobilization of Cyt c on SWNT presented in this work had a good reproducibility. The effects of the thickness of the SWNT film on the electrochemical behavior of the SWNT/GC and Cyt c-SWNT/GC electrode were investigated with voltammetry by adding different microliters of SWNT suspension on electrode surface, for example, 1, 2, 3 and 4 μl. The background currents, i.e., the differences of the currents between the forward scan and backward scan, of the SWNT/GC electrode increased with the increase of the SWNT film thickness. The peak currents of redox reaction of Cyt c, however, were not increased so much as that of the SWNT/GC electrode; the peak currents increased just very slightly with the increase of the thickness of SWNT.

Electrocatalytic activity of Cyt c

It was reported that heme-containing proteins (enzymes), such as Cyt c, myoglobin, and horseradish peroxidase, etc., had an ability to catalyze the reduction of H_2O_2 [64, 65]. To check the electrocatalytic activity of the Cyt c-SWNT/GC electrode to the reduction of H_2O_2, the cyclic voltammetric experiments were performed. Figure 7, curve a and b showed the cyclic voltammograms of the SWNT/GC electrode in 0.1 M PBS (pH 7.0) in the absence (curve a) and presence (curve b) of 5 mM H_2O_2 at a scan rate of 20 mV/s. Curve c was the cyclic voltammogram of the Cyt c-SWNT/GC electrode in PBS containing 5 mM H_2O_2; a large cathodic current for the reduction of H_2O_2 appeared,

and the reduction started at about 0 V. These results indicated that Cyt c kept its electrocatalytic activity after immobilization on the surface of SWNT. The electrocatalytic activity would enable the system to be relatively useful for the development of new bioelectronic nanodevices, for example, enzymes-based biosensors and biofuel cells.

Conclusion

In summary, we had demonstrated in this study by voltammetry and IR spectroscopy that Cyt c remained in its original structure and did not undergo the structural change after being adsorbed on the surface of SWNT. The SWNT-modified electrode showed good promotional effects toward the reduction/oxidation of Cyt c. A pair of redox waves due to the direct electron transfer of Cyt c was obtained. This modified electrode might be used in the development of new biosensors and biofuel cells.

References

 1. Vincent KA, Armstrong FA (2005) Inorg Chem 44:798–809
 2. Fantuzzi A, Fairhead M, Gilardi G (2004) J Am Chem Soc 126:5040–5041
 3. Munge B, Das SK, Ilagan R, Pendon Z, Yang J, Frank HA, Rusling JF (2003) J Am Chem Soc 125:12457–12463
 4. Hudson JM, Heffron K, Kotlyar V, Sher Y, Maklashina E, Cecchini G, Armstrong FA (2005) J Am Chem Soc 127:6977–6989
 5. Gorton L, Lindgren A, Larsson T, Munteanu FD, Ruzgas T, Gazaryan I (1999) Anal Chim Acta 400:91–108
 6. Walcarius A (2001) Electroanalysis 13:701–718
 7. Wang B, Li B, Wang Z, Xu G, Wang Q, Dong S (1999) Anal Chem 71:1935–1939
 8. Bharathi S, Nogami M, Ikeds S (2001) Langmuir 17:1–4
 9. Zimmermann H, Lindgren A, Schuhman W, Gorton L (2000) Chem Eur J 6:592–599
10. Xiao Y, Ju HX, Chen HY (2000) Anal Biochem 278:22–28
11. Cai CX (1995) J Electroanal Chem 393:119–122
12. Zhao GC, Yin ZZ, Zhang L, Wei XW (2005) Electrochem Commun 7:256–260
13. Scott RA, Mauk AG (1995) Cytochrome c—a multidisciplinary approach. University Science Books, Sausalito, CA
14. Murgida DA, Hildebrandt P (2004) Acc Chem Res 37:854–861
15. Taniguchi I, Watanabe K, Tominaga M, Hawkridge FM (1992) J Electroanal Chem 333:331–338

16. Nassar AE, Willis WS, Rusling JF (1995) Anal Chem 67:2386–2392
17. Bowden EF, Hawkridge FM, Chlebowski JF, Babcroft EE, Thorpe C, Blount HB (1982) J Am Chem Soc 104:7641–7644
18. Armstrong FA, Hill HAO, Walton NJ (1988) Acc Chem Res 21:407–413
19. Ion A, Banica FG (2001) J Solid State Electrochem 5:431–436
20. Lojou É, Bianco P (2000) J Electroanal Chem 485:71–80
21. Lojou É, Giudici-Orticoni MT, Bianco P (2005) J Electroanal Chem 579:199–213
22. Patolsky F, Gabriel T, Willner I (1999) J Electroanal Chem 479:69–73
23. Gooding JJ, Wibowo R, Liu JQ, Yang WR, Losic D, Orbong S, Mearns FJ (2003) J Am Chem Soc 125:9006–9007
24. Gooding JJ (2005) Electrochim Acta 50:3049–3060
25. Wang J (2005) Electroanalysis 17:7–14
26. Zhou YK, He BL, Zhang FB, Li HL (2004) J Solid State Electrochem 8:482–487
27. Guo DJ, Li HL (2005) J Solid State Electrochem 9:445–449
28. Shi J, Guo DJ, Wang Z, Li HL (2005) J Solid State Electrochem 9:634–638
29. Wang J, Musameh M, Lin YH (2003) J Am Chem Soc 125:2408–2409
30. Salimi A, Compton RG, Hallaj R (2004) Anal Biochem 333:49–56
31. Rubianes MD, Rivas GA (2003) Electrochem Commun 5:689–694
32. Chen J, Bao J, Cai CX, Lu TH (2004) Anal Chim Acta 516:29–34
33. Chen J, Cai CX (2004) Chin J Chem 22:167–171
34. Musameh M, Wang J, Merkoci A, Yin Y (2002) Electrochem Commun 4:743–746
35. Chicharro M, Sánchez A, Bermejo E, Zapardiel A, Rubianes MD, Rivas GA (2005) Anal Chim Acta 543:84–91
36. Britto PJ, Santhanam KSV, Ajayan PM (1996) Bioelectrochem Bioenerg 41:121–125
37. Chen J, Bao J, Cai CX (2003) Chin J Chem 21:665–669
38. Liang Q, Wang Y, Luo G, Wang Z (2003) J Electroanal Chem 540:129–134
39. Wang M, Shen Y, Liu Y, Wang T, Zhao F, Liu B, Dong S (2005) J Electroanal Chem 578:121–127
40. Yan Y, Zheng W, Zhang M, Wang L, Su L, Mao L (2005) Langmuir 21:6560–6566
41. Cai CX, Chen J (2004) Acta Chim Sinica 62:335–340
42. Cai CX, Chen J (2004) Anal Biochem 325:285–292
43. Patolsky F, Weizmann Y, Willner I (2004) Angew Chem Int Ed 43:2113–2117
44. Guiseppi-Elie A, Lei C, Baughman RH (2002) Nanotechnology 13:559–564
45. Cai CX, Chen J (2004) Anal Biochem 332:75–82
46. Wang J, Li M, Shi Z, Li N, Gu Z (2002) Anal Chem 74:1993–1997
47. Belin T, Epron F (2005) Mater Sci Eng B 119:105–118
48. Lv X, Du F, Ma Y, Wu Q, Chen Y (2005) Carbon 43:2020–2022
49. Lefrant S, Buisson JP, Schreiber J, Chauvet O, Baibarac M, Baltog I (2003) Synth Met 139:783–785
50. Mamedov AA, Kotov NA, Prato M, Guldi DM, Wicksted JP, Hirsch A (2002) Nat Mater 1:190–194
51. Dresselhaus M, Dresselhaus G, Jorion A, Souza-Filho AG, Saito R (2002) Carbon 40:2043–2061
52. Kauppinen JK, Moffatt DJ, Mantsch HH, Cameron DG (1981) Appl Spectrosc 35:271–276
53. Niwa K, Furukawa M, Niki K (1988) J Electroanal Chem 245:275–285
54. Irace G, Bismuto E, Savy F, Colonna G (1986) Arch Biochem Biophys 244:459–469
55. Liu CY, Bard AJ, Wudl F, Weitz I, Heath JR (1999) Electrochem Solid-State Lett 2:577–578
56. Lonetti B, Fratini E, Chen SH, Baglioni P (2004) Phys Chem Chem Phys 6:1388–1395
57. Wang G, Xu JJ, Chen HY (2002) Electrochem Commun 4:506–509
58. Rivas L, Murgida DH, Hildebrant P (2002) J Phys Chem B 106:4823–4830
59. Rikhie J, Sampath S (2005) Electroanalysis 17:762–768
60. Hawkridge FM, Kuwana T (1973) Anal Chem 45:1021–1027
61. Sagara T, Niwa K, Sone A, Hinnen C, Niki K (1990) Langmuir 6:254–262
62. Abass AK, Hart JP (2001) Electrochim Acta 46:829–836
63. Bard AJ, Faulkner LR (2001) Electrochemical methods, fundamental and applications, 2nd edn. Wiley, New York
64. Gu HY, Yu AM, Chen HY (2001) J Electroanal Chem 516:119–126
65. Lei C, Wollenberger U, Bistolas N, Guiseppi-Elis A, Scheller FW (2002) Anal Bioanal Chem 372:235–239